Accepted Manuscript

Synthesis of a series of ethylene glycol modified water-soluble tetrameric TPE-amphiphiles with pyridinium polar heads: Towards applications as light-up bioprobes in protein and DNA assay, and wash-free imaging of bacteria

Vikash Kumar, Viraj G. Naik, Avijit Das, Sourayan Basu Bal, Malabika Biswas, Nupur Kumar, Anasuya Ganguly, Amrita Chatterjee, Mainak Banerjee

PII: S0040-4020(19)30596-4

DOI: https://doi.org/10.1016/j.tet.2019.05.044

Reference: TET 30365

To appear in: *Tetrahedron*

Received Date: 18 April 2019

Revised Date: 14 May 2019

Accepted Date: 21 May 2019

Please cite this article as: Kumar V, Naik VG, Das A, Bal SB, Biswas M, Kumar N, Ganguly A, Chatterjee A, Banerjee M, Synthesis of a series of ethylene glycol modified water-soluble tetrameric TPE-amphiphiles with pyridinium polar heads: Towards applications as light-up bioprobes in protein and DNA assay, and wash-free imaging of bacteria, *Tetrahedron* (2019), doi: https://doi.org/10.1016/j.tet.2019.05.044.

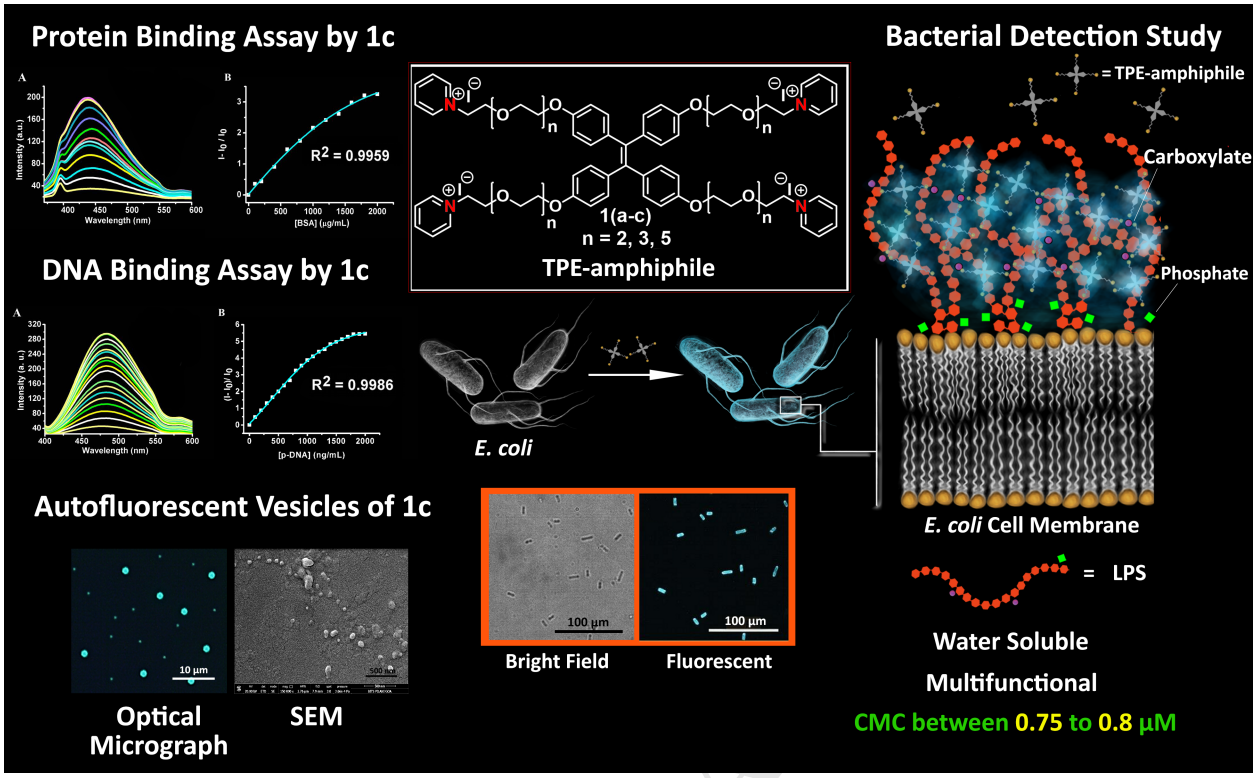

Graphical Abstract

To create your abstract, type over the instructions in the template box below.
Fonts or abstract dimensions should not be changed or altered.

Synthesis of a series of ethylene glycol modified water-soluble tetrameric TPE-amphiphiles with pyridinium polar heads: towards applications as light-up bioprobes in protein and DNA assay, and wash-free imaging of bacteria

Leave this area blank for abstract info.

Vikash Kumar,[a] Viraj G. Naik,[a] Avijit Das,[b] Sourayan Basu Bal,[a] Malabika Biswas,[b] Nupur Kumar,[b] Anasuya Ganguly,[b] Amrita Chatterjee,*[a] and Mainak Banerjee*[a]

[a]*Department of Chemistry, BITS, Pilani, Goa Campus, Goa-403726, INDIA.*
[b]*Department of Biological Sciences, BITS, Pilani, Goa Campus, Goa-403726, INDIA.*

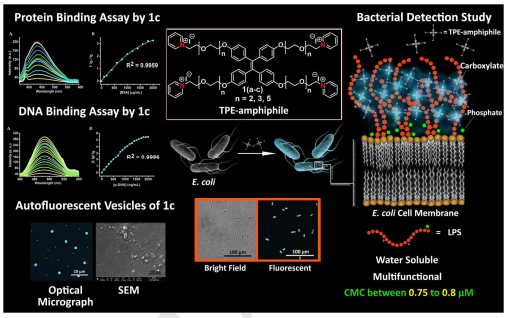

ELSEVIER

Tetrahedron
journal homepage: www.elsevier.com

Synthesis of a series of ethylene glycol modified water-soluble tetrameric TPE-amphiphiles with pyridinium polar heads: towards applications as light-up bioprobes in protein and DNA assay, and wash-free imaging of bacteria

Vikash Kumar, [†,a] Viraj G. Naik, [†,a] Avijit Das,[b] Sourayan Basu Bal,[a] Malabika Biswas,[b] Nupur Kumar,[b] Anasuya Ganguly,[b] Amrita Chatterjee,*[a] and Mainak Banerjee*[a]

[a]*Department of Chemistry, BITS, Pilani, Goa Campus, Goa-403726, INDIA.*
[b]*Department of Biological Sciences, BITS, Pilani, Goa Campus, Goa-403726, INDIA.*

ARTICLE INFO

Article history:
Received
Received in revised form
Accepted
Available online

Keywords:
"Light-up" bioprobes
Tetraphenylethylene (TPE)
Aggregation-induced emission (AIE)
Water-soluble
Protein and DNA binding
Wash-free bacterial imaging

ABSTRACT

Development of water soluble AIE-active "light-up" bioprobes for the detection of biomacromolecules has drawn huge research interests in recent past. In this study, a series of ethylene glycol modified water soluble tetrameric tetraphenylethylene amphiphiles with pyridinium polar heads (TPE-xEG-Py, x = 3, 4, 6 or **1a-c**) have been synthesized by varying the ethylene glycol spacer. Their unique structure allows them to form vesicles and other nanoaggregates in aqueous solutions. These amphiplihes were successfully utilized for fluoremetric detection and quantitation of BSA and DNA based on the electrostatic interactions to trigger AIE-emission from the TPE moiety. The electrostatic interaction was also proved very effective in wash-free imaging of both Gram-negative (*E. coli*) and Gram-positive (*S. aureus*) bacteria with up to 92 folds increase in fluorescence response within bacterial concentration 0–12 x 10^8 CFU mL^{-1}. The strategy is advantageous due to cost-effective and easy synthesis, high water solubility, and fast response.

1. Introduction

Recently fluorescence (FL) detection and imaging of biomacromolecules have attracted great research attention due to requirements in health care and other biomedical applications.[1] Because the FL-based technique offers high sensitivity and selectivity, low background noises, and wide dynamic ranges.[2] In this context, aggregation-induced emission (AIE) based fluorimetric assay has become the most popular approach due to a unique photophysical phenomenon.[3] The AIE-active molecules are non-emissive in the monomeric form in the solution but become highly emissive in the aggregated form due to the restriction of intra-molecular rotations (RIR), which restrict the energy dissipation through the nonradiative decay pathways.[4] This could also address the long-lasting thorny problem of aggregation-caused quenching (ACQ)[5] and make a way to develop efficient chemical and bioprobes.[6]

Tetraphenylethene (TPE), a propeller-shaped compound, is probably the smartest AIE-luminogen reported so far because of its cost-effective synthesis and easy functionalization for various fluorimetric studies.[7] The excellent utility of TPE has been manifested by a vast amount of literature including sensing,[8] bioimaging,[9] light-harvesting materials,[10] mechanochromism[11] and so on.[6] Multifunctional TPE-derivatives are even used for the preparation of supramolecular assemblies.[12] Generally, the AIE property of these probes is modulated by using an organic-water mixed solvent system to display a strong fluorescence output. In the last decade, a series of amphiphilic TPE-derivatives have been reported mostly for the assay and imaging of biomacromolecules.[5b,9] As the assay is usually carried out in water or buffer solutions, water solubility is one of the key requirements of these bio-probes other than biocompatibility. Tang and co-workers have designed a cationic TPE derivative with ammonium polar heads which interacts with proteins and DNAs.[5a] In subsequent years, Tang[13] and Zhang's group[14] have introduced anionic TPE-derivatives for the detection of specific proteins and enzymes. Our group reported a TPE-derivative with sulphonate functionality for selective detection of Gram-positive bacteria.[15] Neutral amphiphiles capable of interacting with biomolecules are also reported. Hu et al. reported a TPE-based glycoconjugate for detection of cholera toxin[16] and another TPE-oligosaccharide by Kato and co-workers is used for the detection of influenza virus.[17] In most of the cases the probe-biomolecule interaction is based on electrostatic or hydrophobic in nature.

Recently, growing interests have been shown in designing of TPE-amphiphiles derived smart nanoaggregates (e.g. vesicles, nanoparticles) because of their multi-targeting and better binding abilities other than unique encapsulation capabilities for better performance in delivery, bioimaging, diagnostics, and theranostics. These amphiphiles can be classified into a) small-molecule amphiphiles,[18] b) amphiphilic polymers,[19] and c)

amphiphilic supramolecules/supramacromolecules.[20] Of our interest, among small-molecule amphiphiles Xia et al. reported a rigid TPE-based bolaamphiphile which form flake-like aggregates in water to emit strong green light.[21] The assembly was utilized for imaging of HeLa cells. Lu and co-workers reported several TPE-based gemini or gemini like amphiphiles with aza-crown ether as the polar head, which spontaneously self-assemble to form micellar aggregates in water and used for gene transfection studies.[22] TPE-based cross-linked autofluorescent vesicles (TPE-CV) have been prepared by Huang et al. in aqueous media which can entrap rhodamine B (RhB) and corresponding TPE-CV@ RhB was used for cell imaging and drug delivery.[23] However, most of these 2nd generation bioprobes involve multistep, complex synthetic strategies and therefore, they are not cost-effective. As one of our focused area of research on TPE-based sensing and imaging systems,[15,24] we envisaged, simple design and cost-effective synthesis of TPE-based amphiphiles, keeping high water solubility and biocompatibility in mind, capable of forming vesicles or other nanoaggregates for multipurpose use in binding assay, wash-free imaging, as staining agent etc. will be a worthy pursuit. The simple design involves incorporation of glycol units of variable lengths in tetrahydroxy-TPE (**3**) for better water solubility and pyridinium polar heads for better biocompatibility. The new series of tetrameric TPE-based amphiphiles (**TPE-xEG-Py**, x = 3, 4, 6 or **1a-c**) showed interesting results on spacer size dependent binding with bio-macromolecules in protein and DNA binding assay as well as detection of bacteria. The best of them (**1c**) was used for wash-free bacterial imaging studies.

2. Results and discussion

*2.1. 2.1 Synthesis and characterization of TPE-amphiphiles (**1a-c**).*

As shown in scheme 1, the TPE-derived bioprobes (**1a-c**) were prepared by attaching four glycol units to tetrahydroxy-TPE (**3**) and then carrying out simple transformations to convert terminal alcoholic groups to corresponding iodides which was finally converted to pyridinium salts by S_N2 mechanism upon heating with pyridine. The first-step involved the McMurry coupling[7a] of 4,4'-dihydroxybenzophenone (**2**) to tetrahydroxy-TPE (**3**). On the other hand, glycols were first monomesylated by treatment with MsCl followed by treatment with sodium iodide to afford glycols with a terminal iodide group (**4a-c**) in good yields. Tetrahydroxy-TPE (**3**) on reaction with monoiodide derivatives of different glycol units (**4a-c**) produced the TPE with four glycol arms, **5a-c** in good yields. These compounds undergo mesylation to give the corresponding products in high yields, which were found to be relatively unstable and were immediately converted to iodide derivative, **6a-c** by refluxing with sodium iodide in high yields over two steps. In the final step, the iodide derivatives, **6a-c** were quarternized by refluxing with excess pyridine in chloroform to produce the desired cationic tetrameric TPE-amphiphiles with pyridinium polar heads (**1a-c**) with iodide as the counter anion in excellent yields.

The structure of this new series of TPE-amphiphiles (**TPE-xEG-Py** or **1a-c**) was established by ^{1}H NMR, ^{13}C NMR, ESI-MS and CHN analysis. The formation of cationic TPE- amphiphiles, **1a-c** from the corresponding iodides **6a-c** was indicated by the appearance of desired number of heteroaromatic protons at downfield within the range δ 8.71-8.25 ppm in ^{1}H NMR, which ensures attachment of pyridine ring for all the TPE-amphiphiles. In addition, the appearance of two carbon (CH) signals at δ ~128.0-128.1 ppm, two carbon (CH) signals at *δ* ~144.7-144.8 ppm and one carbon (CH) signal at *δ* ~145.9-146.0 ppm for each pyridinium ring in ^{13}C NMR spectrum further supported the formation of the desired products. The formation of these TPE-amphiphiles **1a-c** was re-confirmed by ESI-MS (positive ion) mass spectroscopy. In each case, appearance of a base peak at *m/z* = (1/4 x MW-4I) (as *z* = 4) confirmed the formation of tetracationic TPE-amphiphiles. The peaks appeared at 293, 337, and 425 for **TPE-TREG-Py** (i.e. x = 3, **1a**), **TPE-TEG-Py** (i.e. x = 4, **1b**) and **TPE-HEG-Py** (i.e. x = 6, **1c**), respectively. All the spectral studies clearly established the formation of the desired tetrameric TPE-amphiphiles with pyridinium polar heads, **1a-c**.

*2.2 Water solubility, CMC and morphologies of **1a-c***

The tetrameric TPE-amphiphiles, **1a-c** were tested for their aqueous solubility and it was found that all three compounds were highly soluble in water. For each case up to 10 mM aqueous (or buffer) solution was prepared and nominal background fluorescence was observed from up to 0.1 mM of the aqueous solutions which makes them excellent light-up bioprobes. Although background fluorescence increases a little at higher concentrations the solution remains clear which can be seen by naked eyes.

However, the nominal fluorescence shown by these amphiphiles can be beneficial to investigate the self-assembly behaviour of **1a-c** in aqueous solution. It may be assumed that the monomeric units will start self-aggregating at and above a certain concentration which results in increase in fluorescence output from the aqueous solution.[21,22] Accordingly, fluorescence of the aqueous solutions of TPE-amphiphiles, **1a-c** were examined at different lower concentration levels (Fig. S1). The plots of the fluorescence intensity versus corresponding concentrations of **1a-c** are shown in Fig. 1, wherein, inflection points can be located at 0.8 X 10^{-6} mol L^{-1}, 0.77 X 10^{-6} mol L^{-1}, and 0.75 X 10^{-6} mol L^{-1} for TPE-amphiphiles **1a**, **1b**, **1c**, respectively. These inflection points correspond to the critical micelle concentrations (CMCs), where the fluorescence intensity

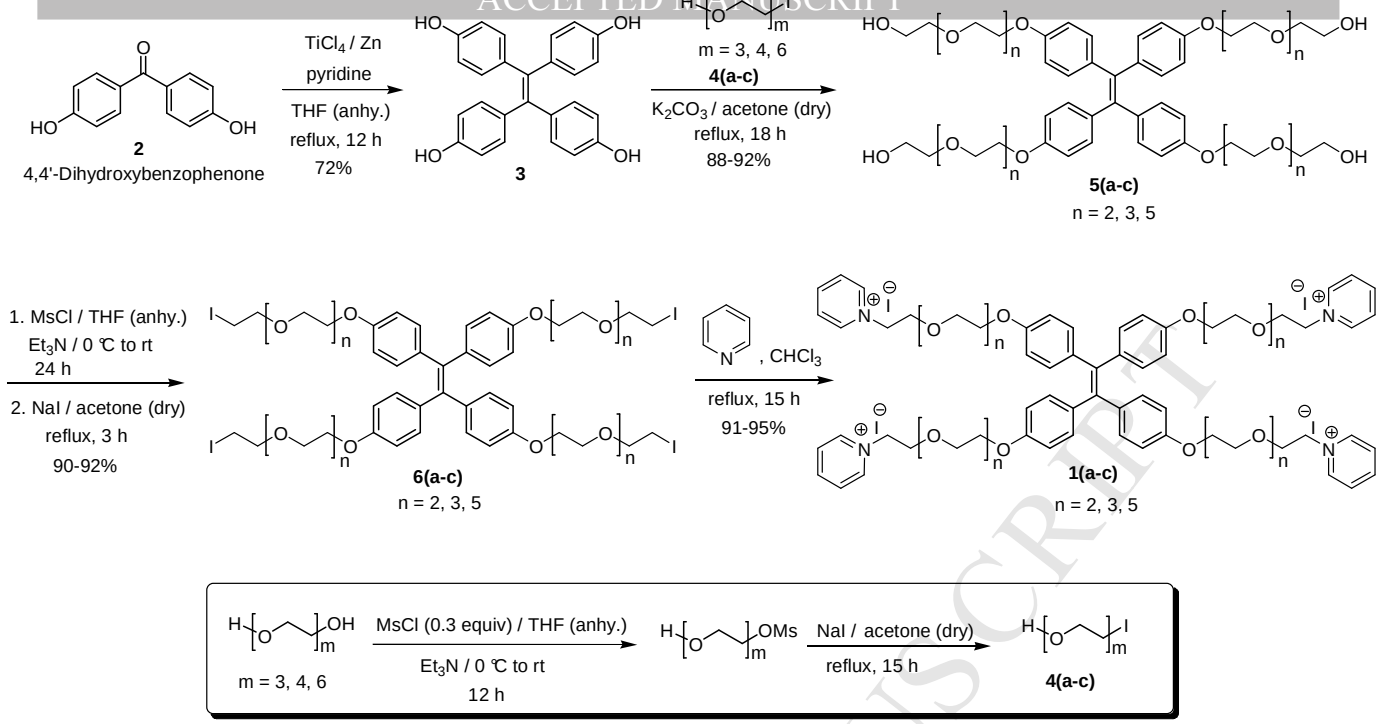

Scheme 1. Synthetic route to the tetrameric TPE-amphiphiles, **1a-c**.

starts increasing due to AIE effect by the formation of nanoaggregates. Similarly, UV-Vis studies were also carried out to reconfirm the CMC values. At lower concentrations, below the CMC values, the absorption spectrum showed two small peaks at 223 and 259 nm but as the concentration was increased, a new peak appeared at 311 nm for all three cases and became stronger with increase in probe concentration (Fig. S1 of SI). The absorbance of other peaks was increased as well. It may be assumed that the small absorption peaks correspond to monomer and the new peak at 311 nm should be attributed to the formation of aggregates in the solution. UV-Vis data gave similar CMC values as that of fluorescence measurements. All the CMC values were in micromolar range and it can be observed that elongation of the chain length in the glycol unit does not have any additional effect on CMC.

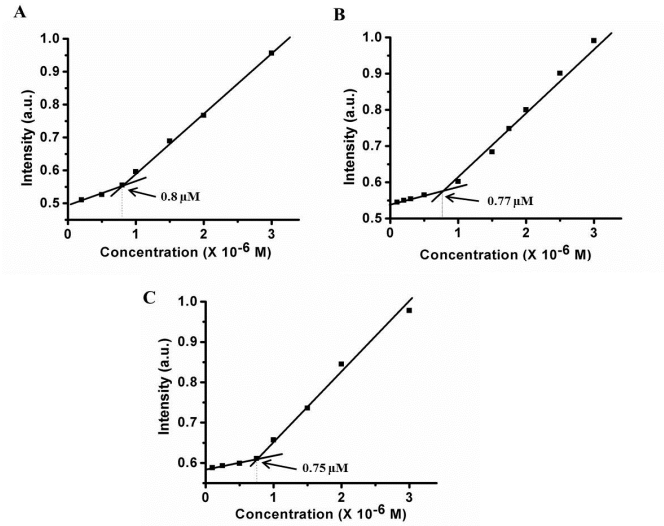

Fig 1. Plots of fluorescence intensity vs concentration of (A) **1a**, (B) **1b** and (C) **1c**, respectively in aqueous solution. The inflection points correspond to CMCs.

It is expected that the four amphiphilic arms of the TPE-amphiphiles, **1a-c** with a hydrophobic TPE moiety at the center would provide a right hydrophobic-hydrophilic balance in the molecules in order to form unique aggregate morphologies in the aqueous solution. The aggregation morphologies of **1a-c** in contact with water were initially investigated under optical micrograph with fluorescence attachment and further confirmed by FE-SEM and DLS analysis (Fig. 2 and Fig. S2, SI). FE-SEM images revealed that all three TPE-amphiphiles spontaneously

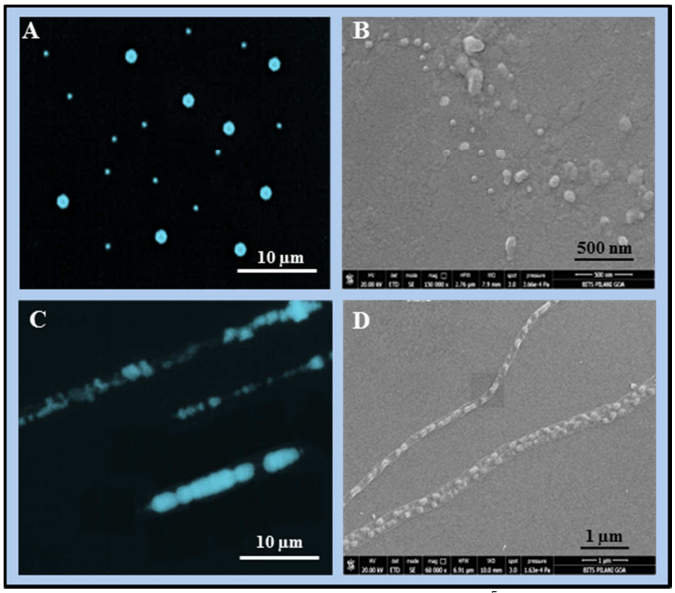

Fig 2. Microscopic images of **1c** in aqueous solution (10^{-5} M): (A) and (C) are the optical micrographs showing formation of fluorescent vesicles and tubes, after aging the solution for 30 min and 1 day, respectively and (B) and (D) are the FE-SEM images at the same condition.

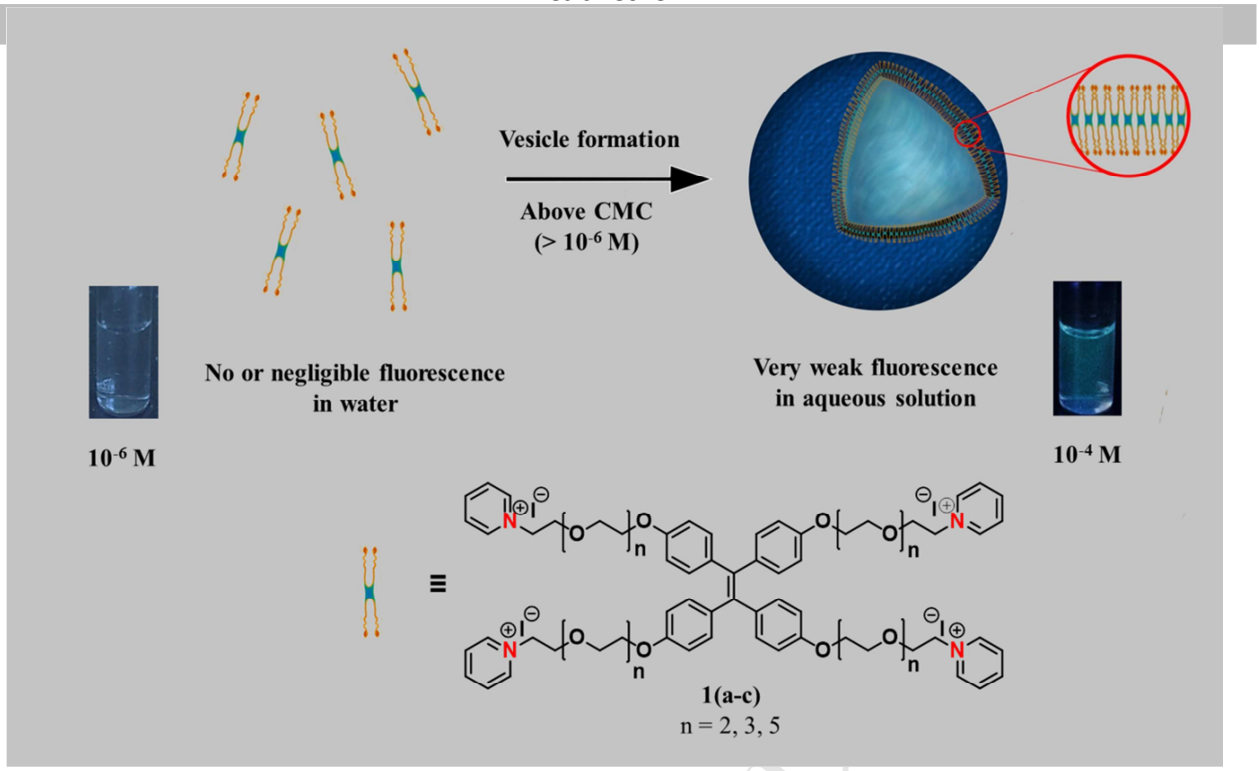

Fig 3. Schematic representation of vesicle formation by tetrameric TPE-amphiphiles, **1a-c**.

form autofluorescent spherical vesicles of variable sizes above their CMCs (10^{-5} M) after incubation of their aqueous solutions for just 30 min (Fig. 2A and Fig. S2A,E, SI). The formation of vesicles was found in FE-SEM analysis as well (Fig. 2B and Fig. S2B,F, SI). Both optical micrograph and FE-SEM further revealed that the spherical vesicles self-aggregate with time to form various unique nano- to micro-sized morphologies. Upon aging the aqueous solutions of **1a** (10^{-5} M) for 1 day formation of rings and short tubular morphologies were observed (Fig. S2C,D, SI). On the other hand, co-existence of vesicles and long tubules were seen for **1b** and long tubes for **1c** upon aging the solutions for just 1 day (Fig. 2C,D and Fig. S2G,H, SI). In a separate study, the particle size of these TPE-amphiphiles **1a-c** in aqueous solution (10^{-5} M) was estimated by DLS analysis after incubation of the samples for 30 min and the results were in coherence with optical micrograph and FE-SEM analysis to re-establish the coexistence of variable sized assemblies. In all cases, narrow ranges of particle size distributions of smaller aggregates as well as bigger aggregates were observed in the similar ranges for these TPE-amphiphiles (Fig. S3, SI). The smaller assemblies found to have average sizes of 60 nm, 59 nm and 69 nm for TPE-amphiphiles **1a**, **1b**, **1c**, respectively; whereas, bigger assemblies of the same appeared at an average diameters of 282 nm, 279 nm and 260 nm indicating spontaneous formation of vesicles. In addition, for **1b** and **1c** a lesser distribution of particles of around 1 μM size were observed in DLS analysis which indicate initiation of the formation of tubular assemblies in the solution. Formation of vesicles is schematically represented in Fig. 3. Presumably, TPE-core with two of the glycolic arms at both sides forms a definite array of lipid monolayer which in turn gets elongated to form monolayer membrane (MLM) vesicles. Quick formation of vesicles and other bigger morphologies is advantageous for better interaction with biomacromolecules.

2.3 Cytotoxicity

Low toxicity of fluorescent bioprobes towards animal cell lines is an essential parameter to test biocompatibility. Cytotoxicity of these TPE-amphiphiles **1a-c** was assessed on HeLa cell line using MTT assay. Live HeLa cells were treated with these amphiphiles at a concentration range 10-100 μM. The percentages of viable HeLa cells were quantified and it was found that cell viability does not alter much for any of the three candidates. The cell viability was more than 90% after 24 h even when the concentration of TPE-amphiphiles was as high as 100 μM in culture medium (Fig. 4). These results also demonstrated that these new TPE-amphiphiles do not cause toxicity to the living human cells.

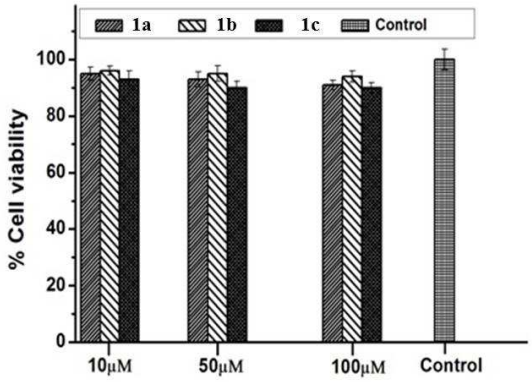

Fig 4. Cytotoxicity study of TPE-amphiphiles **1a-c** on Hela cells by MTT assay.

2.4 Protein binding assay

Application of TPE-amphiphiles **1a-c** as fluorescent bioprobes was explored by analyzing their interactions with bio macromolecules like proteins and DNA. Complexation of the water-soluble TPE based AIE compounds with Bovine serum

albumin (BSA) was investigated by spectrofluorimetric titration in aqueous phosphate buffer (pH = 7.0) at 25 °C (Fig. 5). The experiment was triplicated and similar results were found each time. It was found that the TPE-amphiphiles **1a-c** in buffer solutions (5 µM) in the absence of BSA are almost non-fluorescent, whereas, they show a fluorescence enhancement up to 6-7 folds by the addition of BSA (Fig. 5). The intensity of the probe solution increases up to 2 mg/mL of BSA. A hypsochromic shift from 464 nm (λ_{max} of native probe molecules in phosphate buffer) to 442 nm was observed upon interaction with BSA. The plots display good linear ranges with R^2 values of 0.9959, 0.9976, 0.9959, for **1a**, **1b**, **1c**, respectively. The linear range of $I\text{-}I_0/ I_0$ vs. concentration of BSA plot for **1a** is 0.2 - ~1.2 mg/mL, that of **1b** is 0.4 - ~1.2 mg/mL, and that of **1c** is 0.2 - ~1.2 mg/mL. The studies revealed that all the probes were equally efficient in detecting and quantifying BSA. Notably, the highest enhancement in fluorescence intensity was observed for the probe with six glycol units i.e. **TPE-HEG-Py** (**1c**). As known, the isoelectric point of BSA is at pH 4.5–5.0, therefore, the protein is negatively charged at neutral pH. The fluorescence enhancement may be attributed to the fact that the native folded structures of BSA possess negatively charged regions on the surface and in the pockets, and the positively charged TPE-amphiphiles in the monomeric or aggregated forms bind with them by simple electrostatic interactions, wherein the rotation of the molecules are seized, hence inducing this complex to emit after aggregation.[5a,13] So, AIE property makes the TPE-amphiphiles **1a-c** as efficient probes for protein detection and quantitation.

2.2. 2.5 DNA binding assay

As a part of preliminary investigations on the efficacy of these systems as potential fluorescent probes for DNA and gene delivery, we studied the interaction of these cationic TPE-amphiphiles **1a-c** with plasmid DNA (Fig. 6). pET-28a was used as model plasmid DNA for the spectrometric titration. A dilute solution of TPE-amphiphiles **1a-c** (5 µM) in Tris-EDTA buffer was non-fluorescent. Addition of a small amount of plasmid DNA to the aqueous solution of TPE-amphiphiles (5 µM) turned on its emission. As observed in Fig. 6, increase of the DNA concentrations further increased the fluorescent intensity. Here, the best results were observed for the one with six glycol units (**TPE-HEG-Py**, **1c**) and for other two TPE-amphiphiles the response was relatively lower. The fluorescence intensity of the native probe solution at 478 nm got marginally red shifted to 484 nm upon addition of DNA solution. The change of intensity ($I\text{-}I_0/I_0$) versus concentration of plasmid DNA can be easily fitted to the Boltzman function as shown in (Fig. 6-inset). The plot displays a good linear range from 0.1-1.0 µg with an R^2 value of 0.9987 for **1c**. Thus, TPE-amphiphile **1c** showed good binding efficiency with about 8 folds fluorescence enhancement with plasmid DNA (pET-28a). Similarly for other two amphiphiles viz **TPE-TREG-Py** (**1a**) and **TPE-TEG-Py** (**1b**) enhancement in fluorescence intensity has been observed upon their interaction with p-DNA. However, in both cases the enhancement is not as much as for **1c**. Particularly for **1a** the initial increment is little slow, a saturation point comes after addition of 1.8 µg of DNA. A good linear range of R^2 = 0.9983 was observed from 0.1-1.6 µg. The less response can be attributed to the fact that the nanoaggregates (or the monomers) derived from TPE with shorter glycol units may not have right charge balance or effective length to interact as efficiently as it's congener with six glycol units (i.e **1c**). However, a moderately long **TPE-TEG-Py** (**1b**) offers relatively better binding than **1a** and a linear range was observed from 0.2-1.4 (R^2 = 0.9984) In this case as well, the binding is mainly electrostatic between positively charged TPE derivative and negatively charged DNA. Nonetheless, from the results it may be postulated that a chain length of six glycol units could be the ideal length to interact with DNA better than its congeners. While, the exact reason for this behavior is yet to be established firmly, similar chain length dependent binding affinities for DNA was observed by others.[21] The detection range for DNA is much lower than BSA binding which may be attributed to the fact that the negative charge density on DNA is much higher than BSA to effectively go for stronger electrostatic interactions with the bioprobes.

As TPE-amphiphile **1c** showed excellent results for DNA binding assay, in a demonstration study, it was used as an autofluorescent staining agent for nucleic acids in agarose gel electrophoresis experiment as a potential replacement of conventional dyes. It is worthy to mention that some of the common conventional small-molecule staining agents (e.g. ethidium bromide) are carcinogenic in nature while few others (e.g. nile red) are not adequately photostable. This instigates the search for new staining agents. Gel electrophoresis experiment was carried out in agarose gel (1%) using pET-28a plasmid DNA. It was found that TPE-amphiphile **1c** effectively function as autofluorescent staining agent for pDNA. As shown in (Fig. 6), after binding with the TPE-amphiphile **1c**, DNA bands

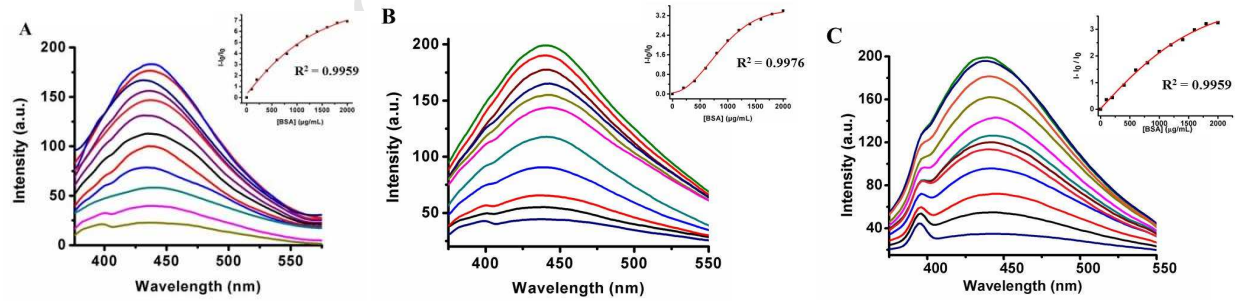

Fig 5. Fluorescence spectra of **1a-c** (5 µM) (A: **1a**; B: **1b**; C: **1c**) upon addition of BSA in an aqueous phosphate buffer (pH = 7.0). Inset: plots of corresponding fluorescence intensities at 442 nm *vs* BSA concentration.

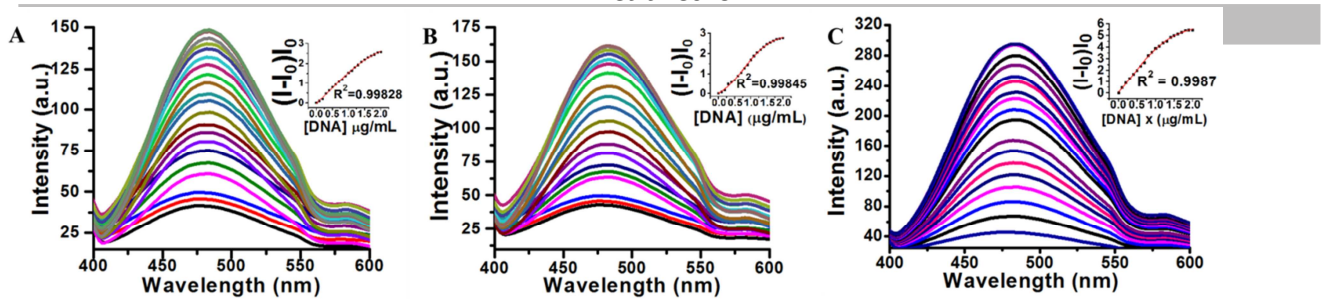

Fig 6. Fluorescence spectra of **1a-c** (5 μM) (A: **1a**; B: **1b**; C: **1c**) upon addition of plasmid DNA (pET-28a) in an aqueous Tris-EDTA buffer. Inset: plots of corresponding fluorescence intensities at 484 nm *vs* DNA concentration.

become visible under UV illumination after a certain concentration of DNA and get intensified with increasing concentration of DNA. It showed fairly good sensitivity as 0.25 μg of plasmid DNA by showing a strong enough band in gel electrophoresis. As expected, positively charged pyridinium units and negatively charged phosphates of DNA strands are mainly involved in the electrostatic interaction leading to the formation of DNA-TPE-amphiphiles conjugates. As the bioprobes, **1c** gets a solid surface in the form of DNA, it light's-up by AIE-effect.

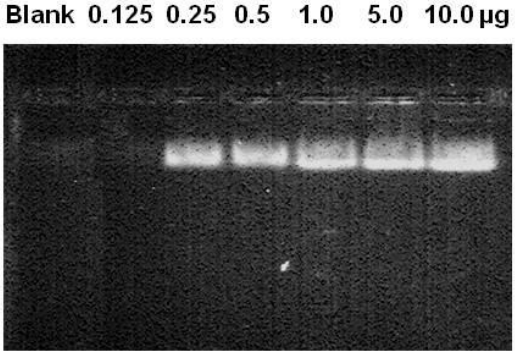

Fig 7. Agarose gel (1%) electrophoresis gel pattern of TPE-amphiphile **1c** (5 μM) – pDNA complex at different concentrations of pET-28a plasmid DNA (0, 0.125, 0.25, 0.5, 1, 5, 10 μg).

2.6 Bacterial detection and wash-free imaging

These TPE-amphiphiles, **1a-c** were also examined as light-up bioprobes for the detection and imaging of various bacterial species. Accordingly, fluorimetric studies were carried out on three different classes of bacteria viz. Gram-negative *E. coli*, Gram-positive *S. aureus* and acid-fast *M. smegmatis* keeping the sensing condition same as in the case of BSA binding and pure water was used as the media. It is presumed that the different negatively charged functionalities available on the cell-walls of bacteria would undergo electrostatic interaction with the positively charged probe molecules to exhibit strong fluorescence from the surface in the same manner as demonstrated by Tang and co-workers.[25] At 10 μM concentration these probes themselves showed little or negligible fluorescence. However, upon incubation of these probes with increasing bacterial concentrations (*E. coli*, *S. aureus*) it led to a gradual increase in fluorescence intensities (Fig. 8 and 9). Bacterial concentration ranges from 2.25 X 10^6 to 12 X 10^8 CFU mL^{-1} for *E. coli* and 3.5 X 10^6 to 12 X 10^8 CFU mL^{-1} for *S. aureus* were screened. The initial bacterial colony formation was estimated from OD of the sample by McFarland standard and the other sample solutions were prepared from it by half dilution method. The interaction of probe molecules with the bacterial surface is very fast as the fluorescence spectra were recorded instantaneously after each addition. It was observed that even after incubation of probe with bacterial solution for 30 min there is hardly any change in the fluorescence output. Although all the probes were capable of interacting with these bacterial surfaces to transmit a strong fluorimetric response with almost equal efficiency, the highest enhancement of fluorescence was observed for probe **1c**. Again, the trend is like the longer the length of the glycol units the better is the interaction with the bacteria. The detection limit **1c**, which is considered here as the lowest concentration at which a fluorescence response is obtained, was estimated to be approximately 9.37 X 10^6 CFU mL^{-1} for *E. coli* (Fig. 8C, inset) and 18.75 X 10^6 CFU mL^{-1} for *S. aureus* (Fig. 9C, inset) with 92 and 38 folds increase in fluorescence intensity from its initial value. Similarly, the detection limits for **1a** and **1b** for *E. coli* and *S. aureus* are estimated to be the same as that of **1c**. Notably, highest enhancement in fluorescence upon interaction with bacterial surface has been observed for **TPE-HEG-Py**, **1c**. A large hypsochromic shift of 76 nm from 476 to 400 nm was observed for *E. coli* in all cases. Similarly a relatively less hypsochromic shift from 476 nm to 422 nm was observed for *S. aureus*. However, no change in fluorescence intensities was observed for *M. smegmatis* (acid-fast) for all three probes. As seen in Fig. 8 and Fig. 9, the probes interact better

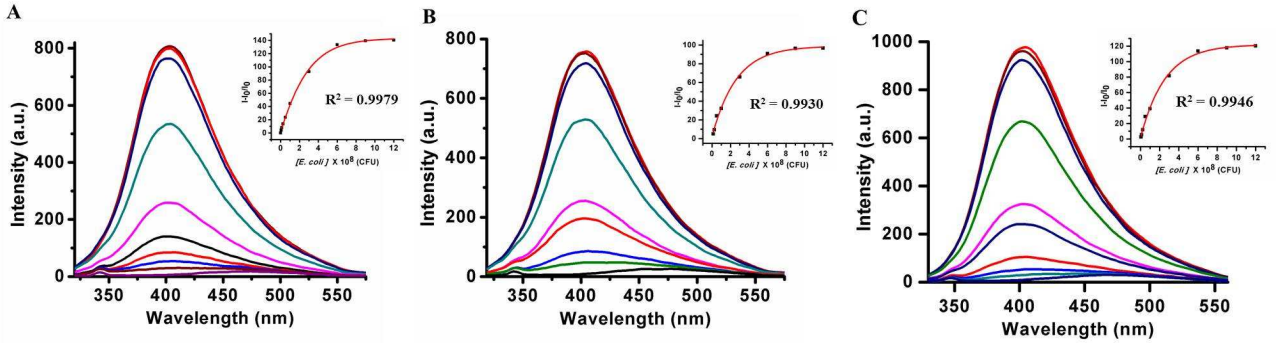

Fig. 8. Fluorescence response of aqueous solution of TPE-amphiphiles **1a-c** (10 μM) [A: **1a**; B: **1b**; C: **1c**] upon addition of increasing concentration of *E. coli*. [λ_{ex} 311 nm; λ_{em} 400 nm]. Inset: plots of corresponding fluorescence intensities against increasing bacterial concentration at λ_{max} 400 nm.

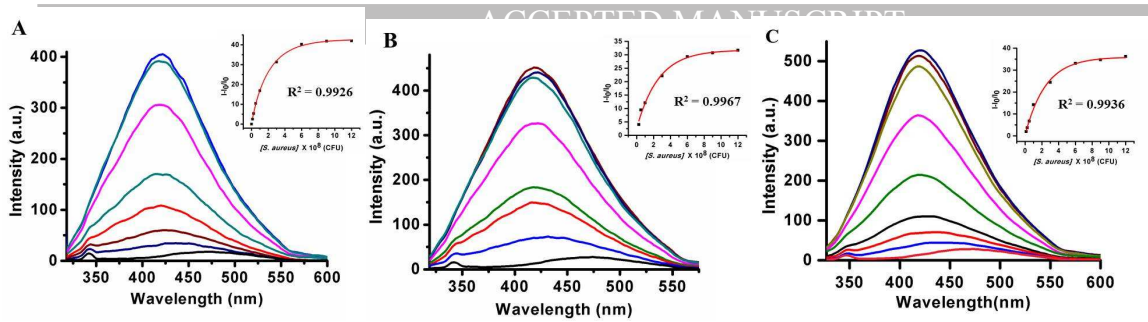

Fig. 9. Fluorescence response of aqueous solution of TPE-amphiphiles **1a-c** (10 µM) [A: **1a**; B: **1b**; C: **1c**] upon addition of increasing concentration of *S. aureus* [λ_{ex} 311 nm; λ_{em} 422 nm]. Inset: : plots of corresponding fluorescence intensities against increasing bacterial concentration at λ_{max} 422 nm.

with *E. coli* than *S. aureus* giving rise to a better fluorescence output. Similarly, the UV-Vis spectra of each solution were recorded and it was observed that all the major bands at around 223, 259 and 311 nm were intensified upon interaction with both bacterial species (see SI, Fig. S4). These experiments unambiguously established the utility of these tetrameric TPE-based probes with pyridine as polar head **(1a-c)** for the detection of both Gram-positive and Gram-negative bacteria. It may be presumed that the bacteria with negatively charged functionality on the cell surface can be efficiently detected by probes **1a-c**.

TPE-amphiphile, **1c** was considered as the best candidate of this series to act as light-up bioprobe for the imaging of various bacterial species. Again for imaging studies the same set of bacteria of three different classes namely *S. aureus*, *E. coli* and *M. smegmatis* were chosen. The higher aqueous solubility with negligible background fluorescence makes **1c** an efficient candidate for wash-free imaging of bacteria. The images were captured under an inverted microscope with fluorescence attachment. Both phase contrast and fluorescence images of *E. coli* were taken by incubating probe **1c** with the bacterial culture for 15 min before capturing images. Similarly, for *S. aureus* 30 min of incubation time was given to intensify the fluorescence output from their cell surface and for *M. smegmatis* images were captured after 1 h. The study revealed that probe **1c** can efficiently interact with the cell-walls of both *E. coli* and *S. aureus* but not with *M. smegmatis* (Fig. 10). For the first two cases i.e. *E. coli* and *S. aureus* an intense blue fluorescence was observed from the bacterial surface, on the contrary, the other bacteria *M. smegmatis* do not show any fluorescence from the cell surface. As there is no requirement of washing of media before imaging, the process remains simple with minimum loss of bacteria. This study once again indicates that probe **1c** can be used as an efficient light-up bioprobe for wash-free imaging of

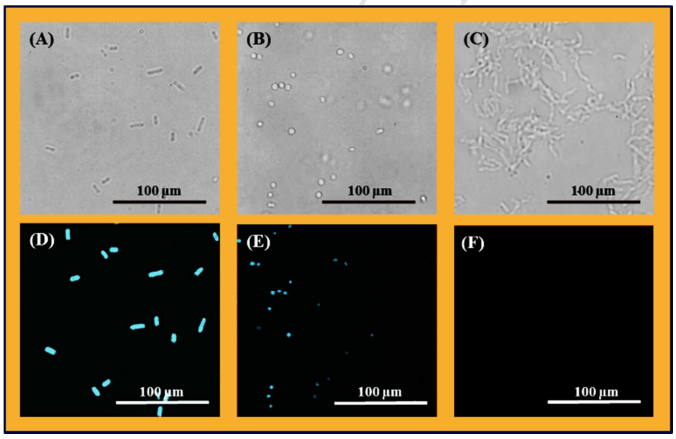

Fig. 10. Phase contrast (A-C) and fluorescence (D-F) images of, *E. coli*, *S. aureus* and *M. smegmatis*, respectively treated with probe **1c** (10 µM). Scale bar for all the images are 100 µm.

both Gram-positive and Gram-negative bacteria. Notably, imaging of *E. coli* by probe **1c** is relatively faster than that of *S. aureus*.

Based on the above results a plausible mechanism for bacterial detection and imaging may be proposed (Fig. 11). The cell surface of *E. coli* possesses LPS (lipopolysaccharides), a characteristic of Gram-negative bacteria, with several carboxylate residues at the outer layer as well as phosphate groups in the backbone. These negatively charged functionalities are easily accessible to the positively charged probe molecules for strong electrostatic interactions. Presumably, the monomers of probe **1c** mostly interact with the cell surface of *E. coli* to form a definitrray of TPE molecules resulting in turn-on type fluorescence response by AIE effect (Fig. 11). Similarly, the deep-seated negatively charged phosphate groups of LTA (lipoteichoic acid) on the cell-wall of the Gram-positive bacteria (viz. *S. aureus*) undergo electrostatic interactions with probe **1c** to exhibit turn-on fluorescence by AIE effect in the same manner like a Gram-negative bacterium (viz. *E. coli*). On the contrary, *M. smegmatis* with mycolic acid, a charge-neutral long chain aliphatic acid, on the cell wall do not effectively interact with the probe molecules and fail to produce any fluorescence response from the cell surface.

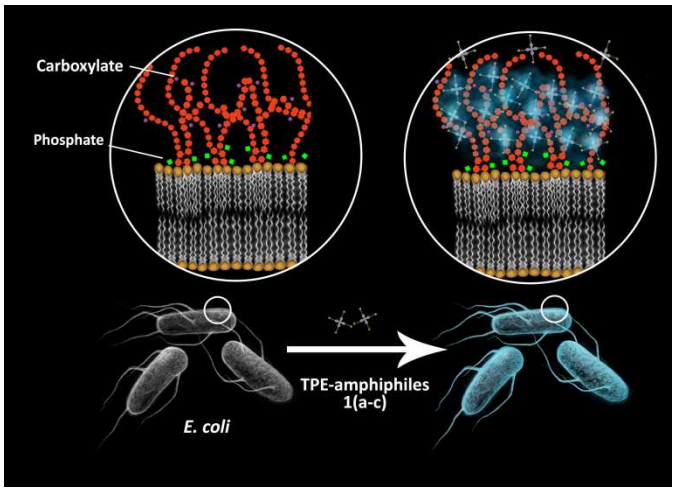

Fig. 11. A schematic representation of the sensing mechanism of bioprobes (**1a-c**) with *E. coli*. The bioprobes undergo simple electrostatic interaction with carboxylates and phosphates groups of LPS seated on the cell-wall of *E. coli* and produce blue fluorescence by AIE-effect.

3. Conclusion

In the present study, a new series of ethylene glycol modified water-soluble tetrameric TPE-amphiphiles with pyridinium polar heads have been synthesized in good overall yields and used for

protein and DNA binding assay, wash-free bacterial imaging, and as staining agents for nucleic acids. They are non-fluorescent in aqueous solution and their CMC values were estimated to be just below micromolar range (0.75-0.8 μM). Their self-aggregation behavior was studied under fluorescence microscope and FE-SEM. They spontaneously form vesicles and other nanoaggregates in aqueous solutions. DLS studies were also conducted to check particle size distribution of the nanoaggregates, which are in well agreement with the microscopic results. MTT assay on HeLa cells revealed that **1a-c** are fairly non-toxic in nature. It was observed that these TPE-amphiphiles **1a-c** bind well with BSA and pDNA (pET-28a) through electrostatic interactions, which turns on fluorescence emission by AIE. Among them TPE-amphiphile with longest glycolic arms, **1c** showed best results. These TPE-amphiphiles, **1a-c** were effectively utilized for wash-free imaging of both Gram-positive (*S. aureus*) and Gram-negative (*E. coli*) bacteria. Presumably, these cationic amphiphiles interact with lipopolysaccharide (LPS) situated at the cell-walls of Gram-negative bacteria (*E. coli*) and lipotiechoic acid (LTA) of Gram-positive (*S. aureus*), and efficiently illuminate them by sitting on their surface. Up to 92 and 38 folds increase in fluorescence was observed for **1c** against *E. coli* and *S. aureus*, respectively, within bacterial concentration 0–12 x 10^8 CFU mL^{-1}. From the results it may be concluded that this new series of TPE-based amphiphiles can be used as multipurpose "light-up" bioprobes for electrostatic interaction based detection and quantitation studies. While the current work focuses on the simple design strategy and cost-effective synthesis of the tetrameric TPE-amphiphile based new bioprobes, and their preliminary applications the advanced applications in drug- and gene-delivery can be considered as future scope of this project.

4. Experimental Section

4.1 General information

4,4′-dihydroxybenzopheneone, various ethylene glycols were purchased from Sigma-Aldrich and used without further purification. $TiCl_4$ was purchased from Spectrochem Pvt. Ltd. Mumbai (India) and Albumin fraction V (from bovine serum) was procured from LOBA Chemie (India). Dulbecco's Modified Eagle's Media (DMEM), Phosphate Buffer Saline (PBS) and MTT (3-(4,5-dimethylthiazol-2-yl)-2,5-diphenyltetrazolium bromide) were purchased from Himedia Laboratories, Mumbai. Plasmid DNA (pET-28a) was purchased from Bangalore GeNei, Bangalore, India. Other common reagents were procured either from SD Fine - Chem Limited, Mumbai, India or from Merck, India and were used without further purification. All ultrapure water used was collected from Millipore water system and purged with N_2 for 15 min prior to use. All the stock solutions of TPE-amphiphiles were prepared by using Tris-EDTA buffer solution or phosphate-buffered saline (PBS) (pH = 7.0) or Milli-Q (18 MΩ) water unless otherwise stated.

4.2 Instruments and measurements

NMR spectra were recorded on BRUKER NMR 300 MHz or 400 MHz systems using tetramethylsilane as an internal standard. Mass spectra were recorded on Waters Q-TOF micro mass spectrometer or Brucker Esquire 3000 mass spectrometer using ESI as the ion source. CHN data were recorded using Vario elementar CHNS analyzer. Agarose gel was viewed under UV transilluminator (BIO-RAD, USA). Fluorescence studies were carried out on a JASCO FP6300 fluorescence spectrophotometer (JASCO Corp., Japan); the slit width was 2.5 nm for both excitation and emission. UV-Visible spectra of probe molecules were taken on a JASCO V-550, the bandwidth and data pitch were set as 1 nm or 5 nm whenever required. Absorbance studies were also carried out on a SHIMADZU UV–2450 UV-visible spectrophotometer (SHIMADZU Corp., Japan) for cytotoxicity assay and for finding optical density of bacterial sample. Optical micrographs were carried out on inverted microscope, IX-51 (Olympus) with fluorescence attachment. Beckman Coulter Delsa Nano particle size analyzer was used for DLS study.

4.3 Materials and methods

4.3.1 General procedure

THF was dried over sodium and freshly distilled before use. The reactions were monitored by thin layer chromatography (TLC) carried out on 0.25 mm silica gel plates (60F-254) using UV light (254 or 365 nm) for visualization. All the stock solutions of TPE-amphiphiles (**1a-c**) were prepared by using Tris-EDTA buffer solution or phosphate-buffered saline (PBS) (pH = 7.0) or deionized water (Milli-Q, 18 MΩ) as per requirements for dilution purpose.

4.3.2 Procedure for agarose gel electrophoresis and cytotoxicity assay

For agarose gel electrophoresis, 0.125, 0.25, 0.5, 1.0, 5.0 and 10.0 μg of plasmid DNA (pET-28a) and 5 μM solution of TPE-amphiphiles (**1a-c**) were mixed so as to make 20 μL volumes and incubated. Then each reaction mixture was loaded on a 1% agarose gel made in tris-acetate-EDTA buffer. After completion of the assay, the gel was viewed under UV transilluminator and photographed.

Cytotoxicity was performed using MTT assay. HeLa cell lines were grown in standard medium as per protocol and they were seeded at a density of 5 x 10^4 cells per well. After 24 h of incubation, the cells were supplemented with TPE-amphiphiles (**1a-c**) at different concentrations. After incubation for 24 h, MTT was added in each well and incubated for 4 h. Finally absorbance was measured after following standard protocol at 570 nm and cell viability was expressed as relative absorbance (%) of the sample vs control cells. The experiments were triplicated and the average data were presented.

*4.3.3 Fluorimetric titration of BSA and p-DNA with TPE- amphiphiles (**1a-c**):*

For fluorescence measurements 1 mM of stock solutions of **1a-c** were prepared in phosphate buffer (pH 7) or deionized water. BSA was dissolved in a pH 7.0 phosphate buffer solution (10.0 mg/mL). DNA was dissolved in Tris-EDTA buffer (1.0 mg/mL) and filtered through a 0.45 μm filter.

Fluorimetric titration for BSA was carried out by adding aliquots of BSA solution in the aqueous phoshate buffer to 10 μL of a 1.0 mM stock solution of TPE-amphiphiles **1a**, **1b** and **1c** followed by adding a measured volume of autoclaved aqueous phosphate buffer (pH 7) to acquire a 2 mL solution. The mixture was stirred for 10 min and then incubated for 10 min at room temperature prior to recording the fluorescence spectrum. All observations were expressed by intensity vs. wavelength plots.

Fluorimetric titration for plasmid DNA was carried out by adding aliquots of p-DNA solution in Tris-EDTA buffer to 10 μL of a 1.0 mM stock solution of TPE-amphiphiles **1a**, **1b** and **1c** in

1.5 mL of Tris-EDTA buffer followed by adding adequate amount of Tris-EDTA buffer to acquire a 2 mL solution (pH 8). The mixture was subjected to vortex for few seconds and then incubated for 10 min at room temperature prior to recording the fluorescence spectrum. All observations were expressed by intensity vs. wavelength plots.

4.3.4 Bacterial sampling

The cultures of different classes of bacteria, namely *E. coli* DH5α, *S. aureus* RN4220 and *M. smegmatis* MC2 155 were selected for the study. These cultures were routinely grown on Luria Bertani broth (Hi-Media, India) for *E. coli*, Tryptic Soy Broth (Becton-Dickinson and Company, USA) for *S. aureus*, and Middlebrook 7H9 broth base (Hi-Media, India) for *M. smegmatis*, respectively. Agar was added as per requirement of routine culture maintenance. At OD_{600} ~0.5 of the grown cells were harvested. OD of bacterial cultures were measured by UV-Visible spectrophotometer and the colony-forming unit (CFU) was obtained by McFarland standards (Table S1, SI).[26] The sample 1 was half-diluted to obtain bacterial samples of lower concentrations.

4.3.5 Procedure for fluorescence and UV-Vis titrations with bacterial stains

1 mM stock solutions of probes were used for the experiments. The grown bacterial cells were harvested by centrifuging at 4 °C, washed twice with sterilized phosphate-buffered saline (1X PBS, pH 7.4) solution and used for fluorescence and UV-Vis measurements. The bacterial cells were re-suspended in 0.9% NaCl solution and the same solution was used for any dilution purpose. The spectra were recorded immediately after mixing probes with bacteria. For fluorescence measurements the excitation wavelength was set to 311 nm and emission spectra were recorded in the range of 312 to 600 nm for **1a-c**. UV-Vis spectra were recorded from 200-800 nm. All the experiments were performed at room temperature.

4.3.6 Wash-free bacterial imaging with phase-contrast and fluorescence microscopy

Cells from overnight grown culture were used to inoculate the secondary culture media and finally the young grown cells were harvested. At OD_{600} ~0.5 of the grown cells were harvested by centrifugation at 4 °C and washed twice with sterilized PBS solution. The washed cells were suspended in an appropriate volume of sterile PBS. Different bacterial sets were prepared with and without probe **1c**, incubated at room temperature for 15 min, 30 min or 1 h as per requirement and directly viewed under an Olympus IX51 inverted microscope, combining the phase-contrast system and the fluorescence system.

*4.4 Synthetic procedures and spectral data of (**1a-c**)*

*4.4.1. Tetra(p-hydroxyphenyl)ethylene **3**:*[7a]

A three-necked flask equipped with a magnetic stirrer was charged with zinc powder (3.1 g, 47 mmol) and 30 mL anhydrous THF under nitrogen atmosphere. The mixture was cooled to 0 to -5 °C and $TiCl_4$ (2.6 mL, 23.5 mmol) was slowly added by a syringe. The suspension was warmed to room temperature and stirred for 30 min, then heated at reflux for 2.5 h. The mixture was again cooled to 0 to -5 °C, charged with pyridine (0.9 mL, 11.3 mmol) and stirred for 10 min. The solution of 4,4′-dihydroxybezophenone (1 g, 4.7 mmol) in 10 mL of THF was added slowly. After addition, the reaction mixture was heated at reflux for 8 h. The reaction was quenched by addition of 10% aqueous K_2CO_3 solution and worked up with $CHCl_3$. The organic layer was collected and concentrated. The crude product was purified by column chromatography using 100-200 silica gel and 2:5 ethyl acetate in petroleum ether (60-80) as an eluent to afford the desired product (**3**). Off-white solid, yield: 72%; ^{1}H NMR (300 MHz, DMSO-d_6): δ (ppm) 6.48 (d, J = 8.4 Hz, 8H), 6.70 (d, J = 8.4 Hz, 8H), 9.22 (s, 4H, exchangeable); ^{13}C NMR (75 MHz, DMSO-d_6): δ (ppm) 114.9, 132.4, 135.5, 138.2, 155.8; ESI-MS: *m/z* 419 $[M + Na]^+$; Anal. Calcd. for $C_{26}H_{20}O_4$: C, 78.77; H, 5.09; Found: C, 78.92; H, 5.11.

*4.4.2. General procedure for the preparation of amphiphilic TPE-glycols (**5a-c**):*

The general procedure is illustrated by the preparation of **5a**.

To a solution of tetra(*p*-hydroxyphenyl)ethylene (**3**, 0.7 g, 1.8 mmol) in dry acetone (7 mL) was added K_2CO_3 (4.88 g, 30.4 mmol) and the reaction mixture was then refluxed for 2 h. Next, monoiodide derivative of triethylene glycol (**4a**) (2.76 g, 10.6 mmol) in dry acetone (10 mL) was added drop by drop in the reaction mixture. The mixture was again refluxed for another 18 h. Then the reaction mixture was filtered and the filtrate was evaporated under vacuum and then the corresponding residue was chromatographed over silica gel (100-200) using 10% MeOH in chloroform to afford the desired compound (**5a**).

*TPE-triethylene glycol **5a***:[27] Colourless sticky thick liquid, yield: 88%; ^{1}H NMR (300 MHz, DMSO-d_6): δ (ppm) 3.48-3.68 (m, 40 H), 3.99 (brs, 8H), 6.69 (d, J = 8.4 Hz, 8H), 6.83 (d, J = 8.4 Hz, 8H); ^{13}C NMR (75 MHz, DMSO-d_6): δ (ppm) 60.3, 67.0, 69.0, 69.8, 72.4, 113.7, 132.1, 136.4, 138.0, 156.8; ESI-MS: *m/z* 925 $[M + H]^+$; Anal. Calcd. for $C_{50}H_{68}O_{16}$: C, 64.92; H, 7.41; Found: C, 65.02; H, 7.44.

*TPE-tetraethylene glycol **5b***:[27] Colourless sticky thick liquid, yield: 89%; ^{1}H NMR (300 MHz, DMSO-d_6): δ (ppm) 3.41-3.54 (m, 48 H), 3.68 (brs, 8H), 4.00 (brs, 8H), 6.69 (d, J = 8.7 Hz, 8H), 6.83 (d, J = 8.7 Hz, 8H); ^{13}C NMR (75 MHz, DMSO-d_6): δ (ppm) 60.7, 67.2, 67.3, 69.4, 70.2, 72.8, 114.1, 132.5, 136.7, 138.4, 157.2; ESI-MS: *m/z* 1123 $[M + Na]^+$; Anal. Calcd. for $C_{58}H_{84}O_{20}$: C, 63.26; H, 7.69; Found: C, 63.38; H, 7.71.

*TPE-hexaethylene glycol **5c***:[27] Colourless sticky thick liquid, yield: 92%; ^{1}H NMR (300 MHz, DMSO-d_6): δ (ppm) 3.49-3.68 (m, 88 H), 3.99 (brs, 8H), 6.69 (d, J = 8.4 Hz, 8H), 6.83 (d, J = 8.4 Hz, 8H); ^{13}C NMR (75 MHz, DMSO-d_6): δ (ppm) 60.3, 67.0, 69.0, 70.0, 72.4, 113.8, 132.1, 136.4, 138.0, 156.8; ESI-MS: *m/z* 1476 $[M + Na]^+$; Anal. Calcd. for $C_{74}H_{116}O_{28}$: C, 61.14; H, 8.04; Found: C, 61.30; H, 8.07.

*4.4.3. General procedure for the preparation of iodide derivatives (**6a-c**) of amphiphilic TPE-glycols (**5a-c**):*

The general procedure is illustrated by the preparation of **6a**.

To a solution of **5a** (0.7 g, 0.76 mmol) in dry THF (7 mL) was added triethylamine (0.92 g, 9.1 mmol) at 0 °C under nitrogen atmosphere. To it mesyl chloride (0.52 g, 4.55 mmol) was added and the mixture was stirred at room temperature for 24 h till the completion of the reaction. Then THF was removed under vacuo and the crude product was diluted with $CHCl_3$ (20 mL) and washed with 5% HCl to remove excess triethylamine. Then the organic extracts were washed with brine, dried over Na_2SO_4 and concentrated. Column chromatogtaphy of the crude product over silica gel (100-200 mesh) eluting with 2% MeOH in $CHCl_3$ afforded the mesylated compound in high yield. The mesylated

compound is relatively unstable and is immediately subjected to iodide formation.

To a solution of mesylated compound of **5a** (0.32 g, 0.26 mmol) in dry acetone (3 mL) was added sodium iodide (0.47 g, 3.10 mmol) under nitrogen atmosphere. The mixture was then refluxed for 3 h. Then the reaction mixture was concentrated *in vacuo* to get crude residue, which was extracted with ethyl acetate (2 x 10 mL). The combined extracts were first washed with 10% $Na_2S_2O_3$ then with brine, dried over Na_2SO_4. Column chromatogtaphy of the crude product over silica gel (100-200 mesh) eluting with 1% MeOH in $CHCl_3$ afforded the desired iodide derivative (**6a**).

TPE-triethylene glycol iodide ***6a***: Colourless sticky thick liquid, yield: 90%; ^{1}H NMR (400 MHz, $CDCl_3$): δ (ppm) 3.24-3.27 (m, 8H), 3.66-3.77 (m, 24H), 3.82-3.84 (m, 8H), 4.05-4.07 (m, 8H), 6.63 (d, *J* = 8.8 Hz, 8H), 6.89 (d, *J* = 8.8 Hz, 8H); ^{13}C NMR (100 MHz, $CDCl_3$): δ (ppm) 3.0, 67.2, 69.9, 70.2, 70.3, 70.6, 70.7, 70.8, 72.0, 113.7, 132.5, 137.0, 138.4, 156.9; ESI-MS: *m/z* 1387 $[M + Na]^+$; Anal. Calcd. for $C_{50}H_{64}I_4O_{12}$: C, 44.01; H, 4.73; Found: C, 43.89; H, 4.75.

TPE-tetraethylene glycol iodide ***6b***: Colourless sticky thick liquid, yield: 91%; ^{1}H NMR (300 MHz, $CDCl_3$): δ (ppm) 3.25 (t, *J* = 6.9 Hz, 8H), 3.67-3.78 (m, 40 H), 3.83 (t, *J* = 4.5 Hz, 8H), 4.04-4.08 (m, 8H), 6.64 (d, *J* = 8.4 Hz, 8H), 6.90 (d, *J* = 8.4 Hz, 8H); ^{13}C NMR (100 MHz, $CDCl_3$): δ (ppm) 2.9, 67.2, 69.8, 70.2, 70.5, 70.6, 70.7, 70.8, 72.0, 113.7, 132.5, 137.0, 138.4, 156.9; ESI-MS: *m/z* 1563 $[M + Na]^+$; Anal. Calcd. for $C_{58}H_{80}I_4O_{16}$: C, 45.21; H, 5.23; Found: C, 45.07; H, 5.26.

TPE-triethylene glycol iodide ***6c***: Colourless sticky thick liquid, yield: 92%; ^{1}H NMR (400 MHz, $CDCl_3$): δ (ppm) 3.22-3.26 (m, 8H), 3.64-3.76 (m, 72 H), 3.79-3.82 (m, 8H), 4.02-4.05 (m, 8H), 6.61 (d, *J* = 8.8 Hz, 8H), 6.87 (d, *J* = 8.4 Hz, 8H); ^{13}C NMR (100 MHz, $CDCl_3$): δ (ppm) 3.0, 67.1, 69.8, 70.2, 70.6, 70.6, 70.7, 70.8, 71.9, 113.6, 132.5, 137.0, 138.3, 156.9; ESI-MS: *m/z* 1893 $[M + H]^+$; Anal. Calcd. for $C_{74}H_{112}I_4O_{24}$: C, 46.94; H, 5.96; Found: C, 47.07; H, 5.98.

*4.4.4. General procedure for the preparation of cationic pyridinium amphiphile of TPE (**1a-c**):*

The general procedure is illustrated by the preparation of **1a**.

To a solution of **6a** (0.2 g, 0.15 mmol) in dry pyridine (1.0 mL) was added dry $CHCl_3$ (2 mL) under nitrogen atmosphere. It was then refluxed for 12 h till the completion of reaction. The reaction mixture was then dried under vacuo to remove $CHCl_3$ and excess pyridine. The residue was re-dissolved in $CHCl_3$ (2 mL) and diethyl ether (10 mL) was added into it to get a light brown coloured crude product as thick oil. The supernatant liquid was decanted and the oily product was subsequently triturated with cold ethyl acetate (2 x 2 mL) followed by cold acetone (2 x 2 mL) to remove any trace of unreacted starting material and pyridine. The sufficiently pure final product was subjected to drying under *vacuo* for several hours to afford tetrameric TPE-amphiphile **1a**.

Bioprobe ***TPE-TREG-Py (1a)***: Light brown sticky liquid, yield: 91%; ^{1}H NMR (400 MHz, D_2O): δ (ppm) 3.49-3.58 (m, 28 H), 3.79-3.92 (m, 20 H), 6.52 (d, *J* = 8.4 Hz, 8H), 6.89 (d, *J* = 8.4 Hz, 8H), 7.84 (t, *J* = 7.0 Hz, 8H), 8.29 ((t, *J* = 7.0 Hz, 4H), 8.71 (d, *J* = 6.0 Hz, 8H); ^{13}C NMR (100 MHz, D_2O): δ (ppm) 61.1, 67.2, 68.7, 68.9, 69.6, 69.9, 114.1, 128.1, 132.4, 137.0, 138.9, 144.7, 146.0, 156.5; ESI-MS: *m/z* 293 (z = 4); Anal. Calcd. for $C_{70}H_{84}I_4N_4O_{12}$: C, 50.01; H, 5.04; N, 3.33; Found: C, 50.15; H, 5.06; N, 3.34.

Bioprobe ***TPE-TEG-Py (1b)***: Light brown sticky liquid, yield: 92%; ^{1}H NMR (400 MHz, D_2O): δ (ppm) 3.41-3.48 (m, 40H), 3.61 (brs, 8H), 3.82-3.85 (m, 16H), 6.47 (d, *J* = 8.6 Hz, 8H), 6.80 (d, *J* = 8.6 Hz, 8H), 7.82 (t, *J* = 7.2 Hz, 8H), 8.27 (t, *J* = 7.9 Hz, 4H), 8.65 (d, *J* = 6.0 Hz, 8H); ^{13}C NMR (100 MHz, D_2O): δ (ppm) 61.0, 67.1, 68.7, 68.9, 68.6, 69.5, 69.8, 113.9, 128.0, 132.4, 136.9, 138.7, 144.7, 145.9, 156.4; ESI-MS: *m/z* 337 (z = 4); Anal. Calcd. for $C_{78}H_{100}I_4N_4O_{16}$: C, 50.44; H, 5.43; N, 3.02; Found: C, 50.61; H, 5.45; N, 3.04.

Bioprobe ***TPE-HEG-Py (1c)***: Light brown sticky liquid, yield: 95%; ^{1}H NMR (400 MHz, D_2O): δ (ppm) 3.47-3.57 (m, 72H), 3.69 (brs, 8H), 3.90-3.91 (m, 16H), 6.54 (d, *J* = 8.0 Hz, 8H), 6.81 (d, *J* = 8.0 Hz, 8H), 7.95-7.99 (m, 8H), 8.44-8.48 (m, 4H), 8.76 (d, *J* = 6.1 Hz, 8H); ^{13}C NMR (100 MHz, D_2O): δ (ppm) 61.1, 67.2, 68.7, 69.0, 69.5, 69.6, 69.8, 114.0, 128.1, 132.4, 136.9, 138.7, 144.8, 146.0, 156.5; ESI-MS: *m/z* 425 (z = 4); Anal. Calcd. for $C_{94}H_{132}I_4N_4O_{24}$: C, 51.09; H, 6.02; N, 2.54; Found: C, 51.23; H, 6.04; N, 2.55.

Acknowledgments

M.B. thanks DST-SERB, India (project no. EMR/2016/002253) and A. C. thanks DST-SERB, India (project no. EMR/2016/001416) for the research fund. V.K. is thankful to CSIR, India for SRFship and V.G.N. thanks DST-SERB for JRFship. The authors also acknowledge central instrumentation facility of BITS-Pilani, Goa campus for FE-SEM. The authors thank Prof. N. N. Ghosh of the same department for the help in DLS measurements.

Conflicts of interest

The authors declare no personal, financial or organizational conflict of interests.

Appendix A. Supplementary data

Supplementary data to this article can be found online at

Notes

∗ Corresponding author 1. MB. Tel.: +91-832-2580-347; fax: +91-832--2557-031; Email: mainak@goa.bits-pilani.ac.in

∗ Corresponding author 2. AC. Tel.: +91-832-2580-320; fax: +91-832--2557-031; Email: amrita@goa.bits-pilani.ac.in

† These authors contributed equally to this work.

References

1. (a) Hong, G.; Antaris, A. L.; Dai, H. *Nat. Biomed. Eng*, **2017**, *1*, 0010. (b) Kim, H. M.; Cho, B. R. *Chem. Rev.* **2015**, *115*, 5014. (c) A Guide to Fluorescent Probes and Labeling Technologies, 10th ed.; Haugland, R. P., Ed.; Molecular Probes: Eugene, **2005**.
2. (a) Chemosensors: principles, strategies and applications, Eds. Wang, B.; Anslyn, E. V. John Wiley & Sons, Inc., 2011. (b) Valeur, B.; Berberan-Santos, M. N. *Molecular Fluorescence: Principles and Applications*, 2nd ed., John Wiley & Sons: New York, **2012**.
3. (a) Tang, B. Z.; Qin, A. Aggregation-Induced Emission:Fundamentals, Wiley, New York, **2013**. (b) Luo, J.; Xie, Z.; Lam, J. W. Y.; Cheng, L.; Chen, H.; Qiu, C.; Kwok, H. S.;

Zhan, X.; Liu, Y.; Zhu,, D.; Tang, B. Z. *Chem. Commun.* **2001**, 1740.

4. Hong, Y.; Lam, J. W. Y.; Tang, B. Z. *Chem. Commun.* **2009**, 4332.
5. (a) Brirks, J. B. Photophysics of Aromatic Molecules, Wiley, London, **1970**. (b) Tong, H.; Hong, Y.; Dong, Y.; Häußler, M.; Lam, J. W. Y.; Li, Z.; Guo, Z.; Guo Z.; Tang, B. Z. *Chem. Commun.* **2006**, 3705.
6. (a) Hong, Y.; Lam, J. W. Y.; Tang, B. Z. *Chem. Soc. Rev*. **2011**, *40*, 5361. (c) Mei, J.; Leung, N. L. C.; Kwok, R. T. K.; Lam, J. W. Y.; Tang, B. Z. *Chem. Rev*. **2015**, *115*, 11718. (d) Wang, Y.; Zhang, G.; Gao, M.; Cai, Y.; Zhan, C.; Zhao, Z.; Zhang, D.; Tang, B. Z. *Faraday Discuss.* **2017**, *196*, 9. (e) He, Z.; Ke, C.; Tang, B. Z. *ACS Omega* **2018**, *3*, 3267.
7. (a) Duan, X. F.; Zeng, J.; Lu, J. W.; Zhang, Z. B. *J. Org. Chem.* **2006**, *71*, 9873. (b) Zhao, E.; Lam, J. W. Y.; Hong, Y.; Liu, J.; Peng, Q.; Hao, J.; Sung, H. H. Y.; Williams, I. D.; Tang, B. Z. *J. Mater. Chem. C* **2013**, *1*, 5661. (c) Feng, G.; Kwok, R. T. K.; Tang, B. Z.; Liu, B. *Appl. Phys. Rev.* **2017**, *4*, 021307. (d) Zhao, Z.; Lam, J. W. Y.; Tang, B. Z. *Curr. Org. Chem.* **2010,** *14*, 2109. (e) Gao, M.; Tang, B. Z. *ACS Sens.* **2017**, *2*, 1382. (f) Yang, Z.; Chi, Z.; Mao, Z.; Zhang, Y.; Liu, S.; Zhao, J.; Aldred, M. P.; Chi, Z. *Mater. Chem. Front.* **2018**, *2*, 861.
8. La, D. D.; Bhosale, S. V.; Jones, L. A.; Bhosale, S. V. *ACS Appl. Mater. Interfaces* **2018**, *10*, 12189.
9. Qian, J.; Tang, B. Z. *Chem* **2017**, *3*, 56.
10. (a) Mei, J.; Leung, N. L. C.; Kwok, R. T. K.; Lam, J. W.Y.; Tang, B. Z. *Chem. Rev.* **2015**, *115*, 11718. (b) Zhao, Y.; He, S.; Yang, J.; Sun, H.; Shen, X.; Han, X.; Ni, Z. *Optical Materials* **2018**, *81*, 102.
11. (a) Zhang, T.; Zhang, R.; Zhao, Y.; Ni. Z. *Dyes and Pigments* **2018**, *148*, 276. (b) Zhang, T. F.; Zhang, R.; Zhang, Z. M.; Ni, Z. H. *RSC Adv.* **2016**, *6*, 79871.
12. (a) Wang, Q.; Li, Z.; Tao, D.-D.; Zhang, Q.; Zhang, P.; Guo, D.-P.; Jiang, Y.-B. *Chem. Commun.* **2016**, *52*, 12929. (b) Feng, H.-T.; Yuan, Y.-X.; Xiong, J.-B.; Zheng, Y.-S.; Tang, B. Z. *Chem. Soc. Rev.* **2018**, *47*, 7452.
13. (a) Tong, H.; Hong, Y.; Dong, Y.; Häußler, M.; Lam, J. W. Y.; Dong, Y.; Sung, H. H. Y.; Williams, I. D.; Tang, B. Z. *J. Phys. Chem. B* **2007**, *111*, 11817. (b) Hong, Y.; Meng, L.; Chen, S.; Leung, C. W. T.; Da, L.-T.; Faisal, M.; Silva, D.-A.; Liu, J.; Lam, J. W. Y.; Huang, X.; Tang, B. Z. *J. Am. Chem. Soc.* **2012**, *134*, 1680.
14. Wang, M.; Gu, X.; Zhang, G.; Zhang, D.; Zhu, D. *Anal. Chem.* **2009**, *81*, 4444.
15. Naik, V. G.; Hiremath, S. D.; Das, A.; Banwari, D.; Gawas, R. U.; Biswas, M.; Banerjee, M.; Chatterjee, A. *Mater. Chem. Front.* **2018**, *2*, 2091.
16. Hu, X. M.; Chen, Q.; Wang, J. X.; Cheng, Q. Y.; Yan, C. G.; Cao, J.; He, Y. J.; Han, B. H. *Chem. Asian J.* **2011**, *6*, 2376.
17. Kato, T.; Kawaguchi, A.; Nagata, K.; Hatanaka, K. *Biochem. Biophys. Res. Commun.* **2010**, *394*, 200.
18. (a) Dong, Y.; Wang, W.; Zhong, C.; Shi, J.; Tong, B.; Feng, X.; Zhi, J.; Dong, Y. *Tetrahedron Lett.* **2014**, *55*, 1496. (b) Xu, L.; Zhu, Z.; Wei, D.; Zhou, X.; Qin, J.; Yang, C. *Appl. Mater. Interfaces* **2014**, *6*, 18344. (c) Hong, Y.; Lam, Häußler, M.; Lam, J. W. Y.; Li, Z.; Sin, K. K.; Dong, Y.; Tong, H.; Lui, J.; Qin, A.; Renneberg, R.; Tang, B. Z. *Chem.–Eur. J.* **2008**, *14*, 6428. (d) Hong, Y.; Xiong, H.; Lam, J. W. Y.; Häußler, M.; Liu, J.; Yu, Y.; Zhong, Y.; Sung, H. H. Y.; Williams, I. D.; Wong, K. S.; Tang, B. Z. *Chem.–Eur. J.* **2010**, *16*, 1232. (e) Noguchi, T.; Shiraki, T.; Dawn, A.; Tsuchiya, Y.; Lien, L. T. N.; Yamamotob, T.; Shinkai, S. *Chem. Commun.* **2012**, *48*, 8090. (f) Wang, X.; Liu, H.; Li, J.; Ding, K.; Lv, Z.; Yang, Y.; Chen, H.; Li, X. *Chem. Asian J.* **2014**, *9*, 784. (g) Zhang, Q.; Liu, Y.-C.; Kong, D.-M.; Guo, D.-S. *Chem. –Eur. J.* **2015**, *21*, 13253. (h) Zhang, M.; Yin, X.; Tian, T.; Liang, Y.; Li, W.; Lan, Y.; Li, J.; Zhou, M.; Ju, Y.; Li, G. *Chem. Commun.* **2015**, *51*, 10210. (i) Kong, Q.; Zhuang, W.; Li, G.; Jiang, Q.; Wang, Y. *New J. Chem.* **2018**, *42*, 9187. (j) Jing, H.; Lu, L.; Feng, Y.; Zheng, J.-F.; Deng, L.; Chen, E.-Q.; Ren, X.-K. *J. Phys. Chem. C* **2016**, *120*, 27577.
19. (a) Zhang, N.; Chen, H.; Fan, Y.; Zhou, L.; Trepout, S.; Guo, J.; Li, M.-H. *ACS Nano* **2018**, *12*, 4025. (b) Zhao, Y.; Zhu, W.; Renb, L.; Zhang, K. *Polym. Chem.* **2016**, *7*, 5386. (c) Zhao, Y.; Wu, Y.; Yan, G.; Zhang, K. *RSC Adv.* **2014**, *4*, 51194. (d) Wang, X.; Yang, Y.; Yang, F.; Shen, H.; Wu, D. *Polymer* **2017**, *118*, 75. (e) Wang, X.; Yang, Y.; Zuo, Y.; Yang, F.; Shen, H.; Wu, D. *Chem. Commun.* **2016**, *52*, 5320. (f) Ma, C.; Chi, Z.; Zhou, X.; Zhang, Y.; Liu, S.; Xu, J. *J. Controlled Release* **2013**, *172*, e14. (g) Zhao, W.; Li, C.; Liu, B.; Wang, X.; Li, P.; Wang, Y.; Wu, C.; Yao, C.; Tang, T.; Liu, X.; Cui, D.; *Macromolecules* **2014**, *47*, 5586. (h) Wang, X.; Yang, Y.; Zhuang, Y.; Gao, P.; Yang, F.; Shen, H.; Guo, H.; Wu, D. *Biomacromolecules* **2016**, *17*, 2920. (i) Guan, X.; Zhang, D.; Jia, T.; Zhang, Y.; Meng, L.; Jin, Q.; Ma, H.; Lu, D.; Laib, S.; Lei, Z. *RSC Adv.* **2016**, *6*, 107622.
20. (a) Liu, Q.; Xia, Q.; Wang, S.; Li, B. S.; Tang, B. Z. *J. Mater. Chem. C* **2018**, *6*, 4807. (b) Li, J.; Liu, K.; Han, Y.; Tang, B. Z.; Huang, J.; Yan, Y. *Appl. Mater. Interfaces* **2016**, *8*, 27987. (c) Zhang, C.-W.; Ou, B.; Jiang, S.-T.; Yin, G.-Q.; Chen, L.-J,; Xu, L.; Lib, X.; Yang, H.-B. *Polym. Chem.* **2018**, *9*, 2021. (d) Li, J.; Liu, K.; Chen, H.; Li, R.; Drechsler, M.; Bai, F.; Huang, J.; Tang, B. Z.; Yan, Y.; *Appl. Mater. Interfaces* **2017**, *9*, 21706. (e) He, L.; Liu, X.; Liang, J.; Cong, Y.; Weng, Z.; Bu, W. *Chem. Commun.* **2015**, *51*, 7148. (f) Li, J.; Shi, K.; Drechsler, M.; Tang, B. Z.; Huang, J.; Yan, Y. *Chem. Commun.* **2016**, *52*, 12466. (g) Chi, X.; Zhang, H.; Vargas-Zúñiga, G. I.; Peters, G. M.; Sessler, J. L. *J. Am. Chem. Soc.* **2016**, *138*, 5829. (h) Zheng, W.; Yang, G.; Jiang, S.-T.; Shao, N.; Yin, G.-Q.; Xu, L.; Li, X.; Chen, G.; Yang, H.-B. *Mater. Chem. Front.* **2017**, *1*, 1823. (i) Ji, X.; Li, Y.; Wang, H.; Zhao, R.; Tangb, G.; Huang, F. *Polym. Chem.* **2015**, *6*, 5021. (j) Liu, Y.-C.; Wang, Y.-Y.; Tian, H.-W.; Liu, Y.; Guo, D.-S. *Org. Chem. Front.* **2016**, *3*, 53.
21. Xia, Y.; Dong, L.; Jin, Y.; Wang, S.; Yan, L.; Yin, S.; Zhou, S.; Song, B. *J. Mater. Chem. B* **2015**, *3*, 491.
22. Zhang, K.-X.; Ding, A.-X.; Tan, Z.-L.; Shi, Y.-D.; Lu, Z.-L.; He, L. *J. Photochem. Photobiol., A* **2018**, *355*, 338. (b) Ding, A.-X.; Tan, Z.-L.; Shi, Y.-D.; Song, L.; Gong, B.; Lu, Z.-L. *ACS Appl. Mater. Interfaces* **2017**, *9* 11546. (c) Ding, A.-X.; Tang, Q.; Gao, Y.-G.; Shi, Y.-D.; Uzair, A.; Lu, Z.-L. *ACS Appl. Mater. Interfaces* **2016**, *8*, 14367.
23. Huang, J.; Yu, Y.; Wang, L.; Wang, X.; Gu, Z.; Zhang, S. *ACS Appl. Mater. Interfaces* **2017**, *9*, 29030.
24. (a) Chatterjee, A.; Banerjee, M.; Khandare, D. G.; Gawas, R. U.; Mascarenhas, S. C.; Ganguly, A.; Gupta R.; Joshi, H. *Anal. Chem.* **2017**, *89*, 12698. (b) Khandare, D. G.; Joshi, H.; Banerjee, M.; Majik, M. S.; Chatterjee, A. *Anal. Chem.* **2015**, *87*, 10871. (c) Chatterjee, A.; Khandare, D. G.; Saini, P.; Chattopadhyay, A.; Majik, M. S.; Banerjee, M. *RSC Adv.* **2015**, *5*, 31479. (d) Khandare, D. G.; Joshi, H.; Banerjee, M.; Majik, M. S.; Chatterjee, A. *RSC Adv.* **2014**, *4*, 47076. (e) Khandare, D. G.; Kumar, V.; Chattopadhyay, A.; Banerjee, M.; Chatterjee, A. *RSC Adv.* **2013**, *3*, 16981.
25. Zhao, E.; Chen, Y.; Chen, S.; Deng, H.; Gui, C.; Leung, C. W.; Hong, Y.; Lam, J.W.; Tang, B. Z. *Adv. Mater.* **2015**, *27*, 4931.
26. McFarland, J. *J. Am. Med. Assoc.* **1907**, *49*, 1176.
27. Song, S.; Zheng, H. F.; Li, D. M.; Wang, J. H.; Feng, H. T.; Zhu, Z. H.; Chen, Y. C.; Zheng, Y. S. *Org. Lett.* **2014**, *16*, 2170.

Highlights

- A series of ethylene glycol modified TPE with pyridinium polar heads is synthesized
- The AIE-active “light-up” probes are water-soluble and nonfluorescent in solution
- They spontaneously form vesicles and other nanoaggregates in aqueous solution
- The bioprobes are biocompatible and used for protein and DNA binding assay
- They were effectively used in wash-free imaging of bacteria and as staining agent